OBSERVATIONS OF ULTRAVIOLET EMISSION LINES IN SOLAR CORONAL HOLES ON THE DISK WITH SUMER ON SOHO

Klaus Wilhelm,[1] Ingolf E. Dammasch[1], and Lidong Xia[1]

[1] *Max-Planck-Institut für Aeronomie, Max-Planck-Straße 2, 37191 Katlenburg-Lindau, Germany*

ABSTRACT

The Solar Ultraviolet Measurements of Emitted Radiation (SUMER) spectrograph and other instruments on the Solar and Heliospheric Observatory (SOHO) have observed many solar polar coronal holes (PCHs) during the minimum of the sunspot cycle in 1996 and 1997. Based on the results obtained for PCHs, investigations of near-equatorial coronal holes (ECHs) have been planned and carried out at the beginning of the new sunspot cycle, when ECHs regularly occurred on the solar disk. These studies have been performed using ultraviolet emission lines with formation temperatures ranging from 20 000 K to one million kelvin as well as continuum radiation. The spectroscopic evaluation provides information on line shifts and widths, and on the dynamics of the low corona in coronal holes (CHs). The characteristics of ECHs found are very similar to those of PCHs observed during the sunspot minimum. Specifically, we find outflow speeds of Ne^{7+} ions of about 5 km s^{-1} and of Mg^{8+} ions of 15 km s^{-1} with respect to quiet-Sun (QS) regions. The Doppler widths of the Mg IX (λ706) line inside ECHs and in the QS are not significantly different and correspond to $v_{1/e} \approx 60$ km s^{-1}.

INTRODUCTION

The significance of CHs for the interaction of the solar magnetic field and the upper atmosphere with the interplanetary space has been demonstrated over the last decades by many space missions. Of particular importance is the fact that the fast solar wind is generated within CHs (Krieger et al., 1973). Ulysses observations have shown that the PCHs are the sources of fast solar wind streams during the sunspot minimum (Geiss et al., 1995; Woch et al., 1997). The instruments on SOHO – launched in December 1995 near the minimum of the magnetic activity of the Sun – made possible detailed studies of the PCHs and the sources of the fast solar wind (e.g., Insley et al., 1997; DeForest et al., 1997; Kohl et al., 1997, 1999a,b; Antonucci et al., 1997; Wilhelm et al., 1998, 2000; David et al., 1998; Hassler et al., 1999; Stucki et al., 1999; Fludra et al., 1999; Wilhelm, 1999; Cranmer et al., 1999; Giordano et al., 2000). The outflow of hydrogen and minor ions as tracers of the solar wind could be followed from the lanes of the chromospheric network out to several solar radii. A rapid acceleration to the asymptotic solar wind speed was found together with a high temperature of the ions perpendicular to the magnetic field direction and a low electron temperature. The geometry in PCHs is not ideal for Doppler measurements of bulk speeds as the line-of-sight (LOS) component is expected to be only a fraction of the total speed. ECHs should provide better viewing conditions in this respect. It is also of considerable interest to explore whether there are systematic differences between the characteristics of polar and near-equatorial CHs. During the sunspot minimum, ECHs were very rare features, but initial studies could be performed. Del Zanna and Bromage (1999) found electron densities and temperatures in ECHs comparable to those in PCHs and also similar plume characteristics. Lemaire et al. (1999) measured larger Doppler widths of transition region lines in ECHs than in quiet-Sun regions. With increasing solar activity in sunspot cycle 23, the existing large PCHs disintegrated and smaller CHs formed more often away from the poles, which we will call here ECHs. Spectroscopic and morphological studies of such ECHs with the help of ultraviolet emission lines are the main topic of this communication.

Table 1. Observational parameters of some of the CH images. A slit with angular dimensions of 1″× 300″ (1″ corresponds to ≈ 715 km at the Sun) and an exposure time of 150 s were used in all cases. Note that the solar rotation during the observations affects the field of view. Spectroheliograms of lines in parentheses are not shown, but all studies can be found with line profiles at http://www.linmpi.mpg.de/english/projekte/sumer/text/ech99.html.

Date 1999	Time UT	Solar coordinates $x_\odot$ / ″	Solar coordinates $y_\odot$ / ″	Emission lines and continua	Steps / ″	Detector
12 June	18:01 – 23:54	11 E – 251 W	376 S – 676 S	(O II), (O III), (Ar VIII), Mg IX, C	1.88	B
19 Oct.	08:54 – 14:57	489 E – 327 E	282 N – 18 S	(H I), (He II), (C)	1.13	A
19 Oct.	15:00 – 21:03	439 E – 277 E	270 N – 30 S	He II, (N II), C	1.13	A
3/4 Nov.	18:50 – 00:25	469 E – 70 E	60 S – 360 S	(Si II), C IV, Ne VIII, C	3.0	A
07 Nov.	00:05 – 10:08	19 E – 700 W	400 S – 100 S	(Si II), (C IV), (Ne VIII), (C)	3.0	A

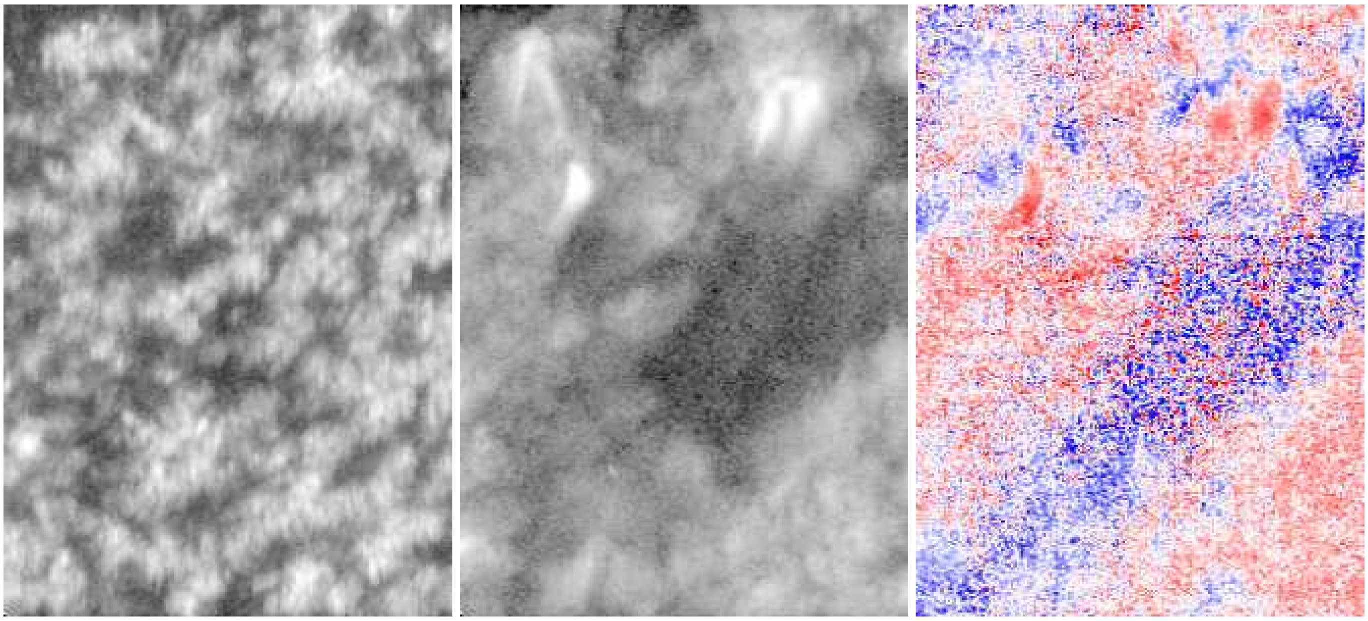

Fig. 1. Raster scans of an area covering a small CH on the disk embedded in QS regions on June 12, 1999. On the left, the continuum intensity is shown near 710 Å. The Mg IX (λ706) line is displayed in intensity (middle) and Doppler shift (right; full scale: ± 30 km s^{-1}). The dimensions of the images are 221″ × 300″.

INSTRUMENTATION AND OBSERVATIONS

The SUMER spectrograph was used to obtain the observations to be discussed. The instrument and its performance has been presented in detail elsewhere (Wilhelm et al., 1995, 1997; Lemaire et al., 1997). The observational parameters are compiled in Table 1 where a selection of CH studies on the disk is given. In our list, the line with the highest formation temperature of 950 000 K is Mg IX. Lines with higher formation temperatures (e.g., Mg X at 1.1 × 10^6 K) were so dark in CHs that reliable Doppler measurements could not be obtained. In addition to the emission lines, the continuum radiation was also evaluated in order to display the chromospheric network at the lowest height levels that can be observed with SUMER. In Figure 1 we show spectroheliograms of the continuum near 710 Å and the Mg IX (λ706) line covering a small CH. The chromospheric network is well defined in the H I Lyman continuum (and also in O II and O III) both inside and outside of the CH. Small loop-like elements seem to straddle the network lanes. In Ar VIII (formation temperature: 400 000 K) the network is more fuzzy in QS regions and darker in the CH. In Mg IX the CH is very dark and the network is nearly absent in QS regions, but large loop structures are visible.

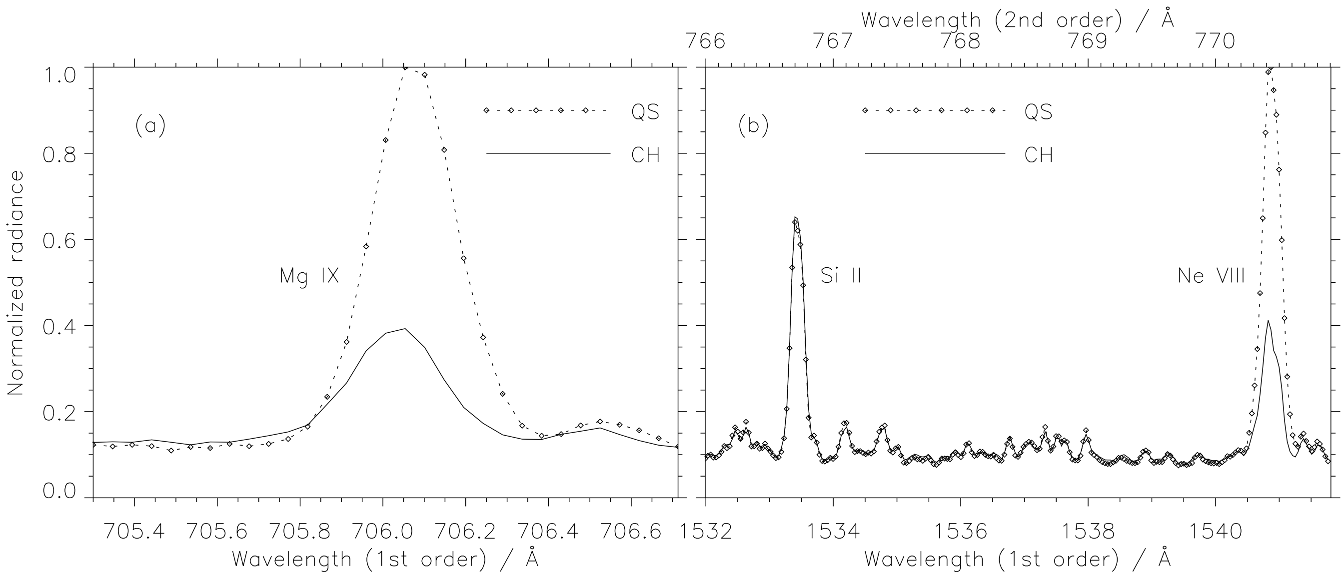

Fig. 2. (a) Spectral profiles of the Mg IX (λ706) emission line for CH and QS conditions. (b) Spectra showing the Si II (λ1533) line (in first order) and Ne VIII (λ770) line (in second order) inside and outside of ECHs. The spectra are normalized to the peak QS values. CH spectra are shown on the same scale. The CH has no effect on Si II and the continuum compared to QS conditions.

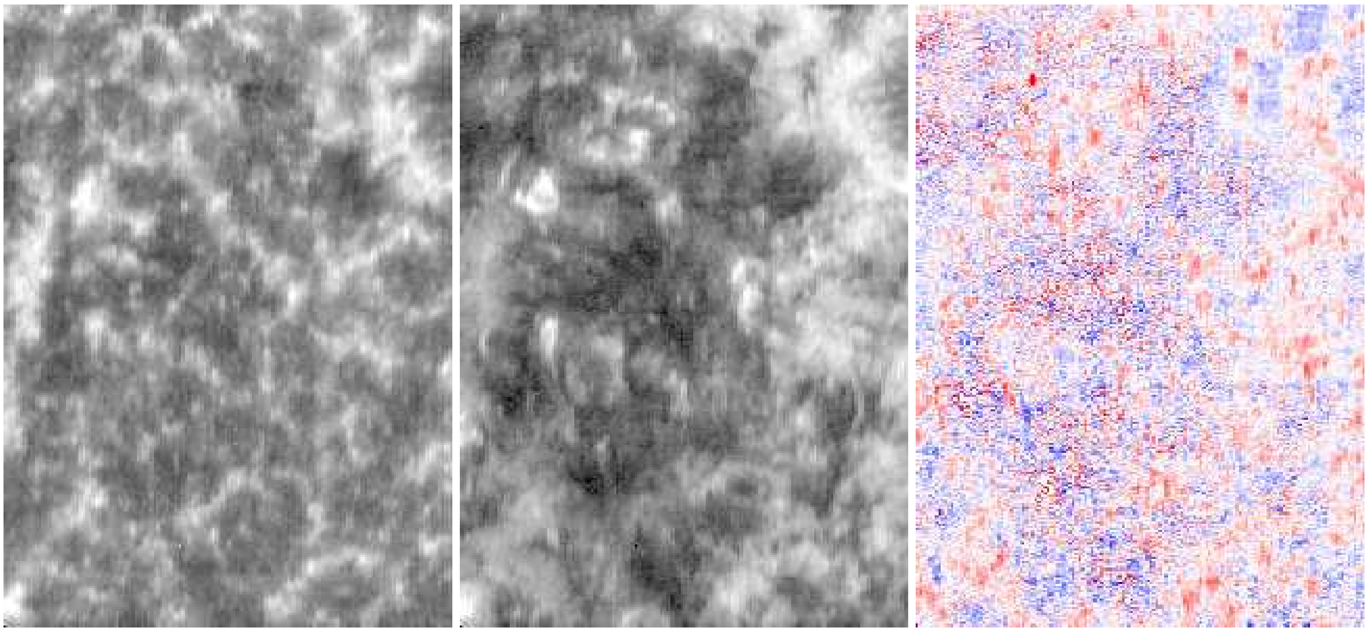

Fig. 3. Raster images of a small CH in He II (λ1085) (intensity: middle; Doppler shift: right; full scale: $\pm$ 30 km s^{-1}) and the continuum near 1087 Å (left) obtained on October 19, 1999. The dimensions of the images are $215'' \times 300''$. QS regions can be seen in the western portion of the scan.

The dark area in Mg IX can also be identified as a CH region in all windows from He II to Fe XV of the Extreme-ultraviolet Imaging Telescope (EIT; Delaboudinière et al., 1995). Reliable line-shift measurements could be performed for O II, O III and Mg IX. The transition region lines are predominantly shifted towards red in the bright network lanes and blue in the dark cell areas. The Dopplergram of the coronal line Mg IX is also displayed in Figure 1. It is blue inside the CH indicating an outward flow. In an attempt to quantify this shift, average profiles of the line inside and outside of the CH are plotted in Figure 2(a). We find an average LOS blue shift of –15 km s^{-1} in the CH with respect to the QS (–12 km s^{-1} relative to O II, but, considering the uncertainties involved, we do not claim that the difference is significant), and a Doppler width of λ_D = 151 mÅ ($v_{1/\mathrm{e}}$ = 64 km s^{-1}) compared to 143 mÅ (61 km s^{-1}) in QS regions. Outside the CH red shifts are more common; in particular, the brightest loop structures are characterized by strong downflows.

On October 19, 1999 observations were performed in a CH near the equator east of the central meridian. Again the CH was very clearly defined in all EIT channels. Some of the observations are presented in Figure 3. In the continuum near 1087 Å and in the N II (λ1084) line, we see the network without significant changes across CH boundaries. The H I Ly δ line is darker within the CH and the He II ($\lambda\lambda$958, 1085) Balmer lines are much darker inside the CH than outside, but display some structure related to the network. Red shifts in the Dopplergrams and an increase in line widths are correlated with bright features of the corresponding emission lines in the QS regions and the CH.

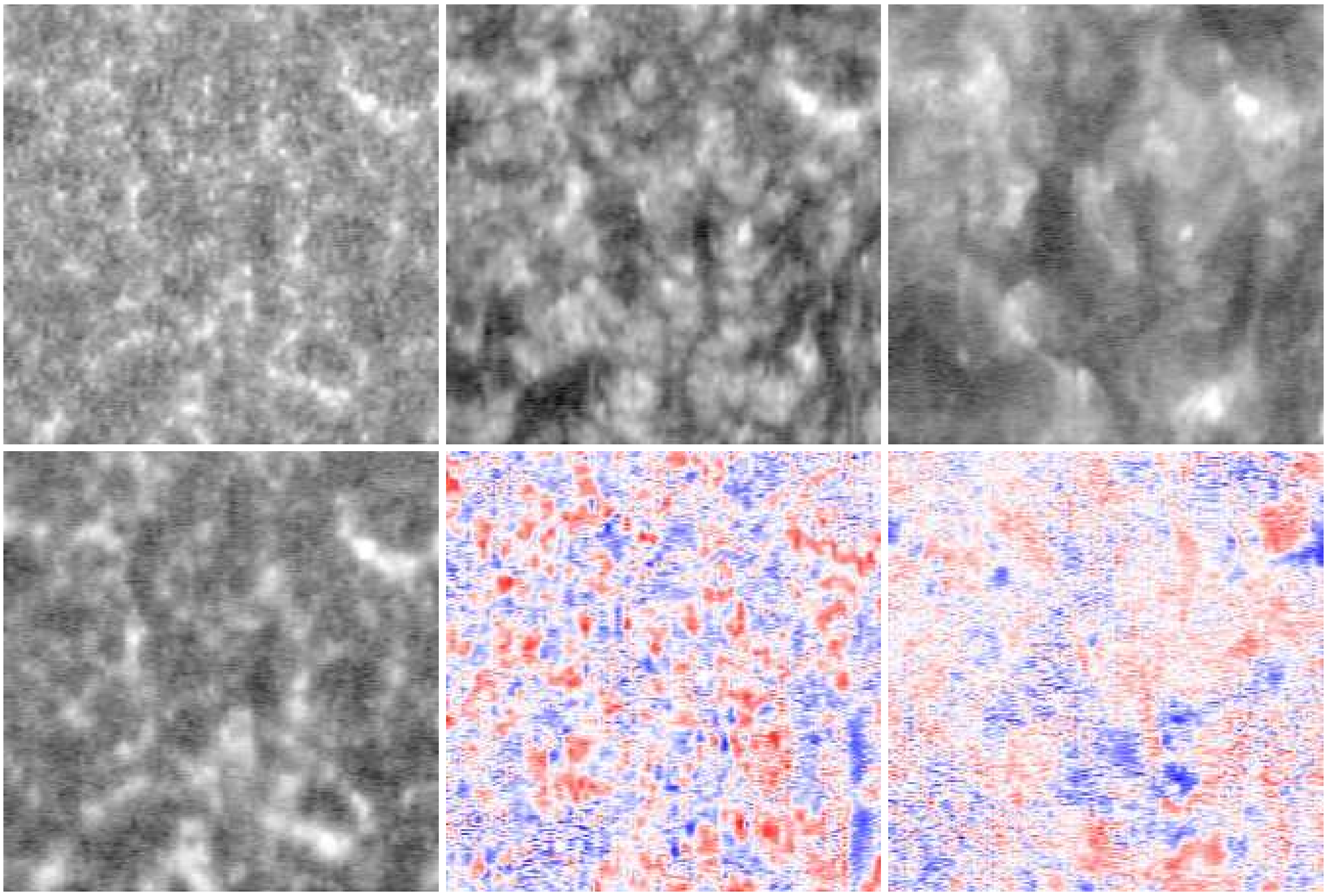

Fig. 4. Simultaneous raster scans in continuum radiation near 1540 Å (top left), in the C IV (λ1548) line (top middle), and in the Ne VIII (λ770) line in second order (top right) observed on November 3, 1999. The Si II (λ1533) line (bottom left) is also shown from the same scan as well as the Doppler shifts (full scale: ± 30 km s^{-1}) for C IV (bottom middle), and Ne VIII (bottom right). The dimensions of the images as shown are 222″ × 225″.

In contrast to the CHs discussed above, the CH on November 3, 1999 is only prominent in the Fe XII and Fe XV channels of EIT. There are some indications of a CH in the Fe X/XI window and in He II, but it is obvious that there are many closed magnetic loops containing plasma of $\approx 1 \times 10^6$ K. As a consequence, we find no clear CH signature in the Ne VIII line. This can be seen from Figure 4 where the intensity images of C IV, Ne VIII, and Si II are displayed together with the thermal continuum near 1540 Å. The continuum outlines the network quite well (as does the Si II line at 1533 Å). Network bright points are aligned along the network lanes. Some of them can also be seen in C IV and Ne VIII, however, with less structural details at higher line formation temperatures. An evaluation of the line shifts (shown for C IV and Ne VIII) revealed that there is a very good correlation between bright areas in C IV and red shifts, but for Ne VIII the situation is rather complex.

The last case to be discussed, is a large CH on November 7, 1999. It is reasonably well defined in Fe XII and Fe XV, but the He II and Fe IX/X windows exhibit CH signatures only in a restricted area. In this region the Ne VIII line is very dark and shifted towards blue by –5 km s^{-1} relative to the QS wavelength. Spectra are shown in Figure 2(b). For the evaluation of the shift, procedures were used similar to those outlined by Dammasch et al. (1999), and the result obtained is in agreement with outflow speeds of Ne VIII in PCHs.

DISCUSSION AND CONCLUSIONS

All ECHs presented here were very clearly defined in the hot iron lines of EIT, but only two of them displayed other typical CH signatures (low emission above 600 000 K and in He II; blue shift in coronal lines) over their complete area. The implications of this distinction are under study. If we restrict our remarks to those regions where the CH was fully developed, the following conclusions can be drawn: outflow can be detected for lines with formation temperatures above 100 000 K. An average outflow speed of –5 km s^{-1} can be seen in Ne VIII (600 000 K); the outflow increases to more than 10 km s^{-1} in absolute speed for Mg IX (950 000 K). The radiance ratios decrease with the formation temperature from $L(\mathrm{CH})/L(\mathrm{QS}) = 1$ in the continuum to ≈ 0.3 for Mg IX. The decrease sets in at a temperature of about 100 000 K. No systematic variations of the line widths could be found with the present data set. The lack of Mg X emission indicates an electron temperature not higher than 1×10^6 K. All CHs studied do not influence the brightness and the structure of the chromospheric network in the continua and the Si II and O II lines. In summary, ECHs appear to have characteristics very similar to those of PCHs.

It should be pointed out that all transition region lines exhibit a strong positive correlation between brightness and red shift as well as line width in CH and QS regions. Finally, it is worth mentioning that the network morphology is fundamentally different if seen in the continuum near 710 Å or near 1540 Å. The H I Lyman continuum shows many small loop-like features (cf., Feldman et al., 2000), whereas in the thermal continuum the network lanes are outlined by network bright points at the limit of the instrumental spatial resolution.

ACKNOWLEDGEMENTS

The SUMER project is financially supported by DLR, CNES, NASA and the ESA PRODEX Programme (Swiss contribution). SOHO is a spacecraft mission of international co-operation between ESA and NASA.

REFERENCES

Antonucci, E., G. Noci, J. L. Kohl, G. Tondello, M. C. E. Huber, et al., First Results from UVCS: Dynamics of the Extended Corona, in ASP Conf. Ser., **118**, 273-277, 1997.

Cranmer, S. R., G. B. Field, and J. L. Kohl, Spectroscopic Constraints on Models of Ion Cyclotron Resonance Heating in the Polar Solar Corona and High-Speed Solar Wind, *Astrophys. J.*, **518**, 937-947, 1999.

Dammasch, I. E., K. Wilhelm, W. Curdt, and D. M. Hassler, The Ne VIII (λ770) Resonance Line: Solar Wavelengths Determined by SUMER on SOHO, *Astron. Astrophys.*, **346**, 285-294, 1999.

David, C., A. H. Gabriel, F. Bely-Dubau, A. Fludra, P. Lemaire, and K. Wilhelm, Measurement of the Electron Temperature Gradient in a Solar Coronal Hole, *Astron. Astrophys.*, **336**, L90-L94, 1998.

DeForest, C. E., J. T. Hoeksema, J. B. Gurman, B. J. Thompson, S. P. Plunkett, et al., Polar Plume Anatomy: Results of a Coordinated Observation, *Solar Phys.*, **175**, 393-410, 1997.

Delaboudinière, J.-P., G. E. Artzner, J. Brunaud, A. H. Gabriel, J. F. Hochedez, et al., EIT: Extreme-Ultraviolet Imaging Telescope for the SOHO Mission, *Solar Phys.*, **162**, 291-312, 1995.

Del Zanna, G., and B. J. I. Bromage, Characterization of Solar Coronal Holes and Plumes Using Spectroscopic Diagnostic Techniques Applied to SOHO/CDS Observations, *Space Sci. Rev.*, **87**, 169-172, 1999.

Feldman, U. , I. E. Dammasch, and K. Wilhelm, The Morphology of the Solar Upper Atmosphere During the Sunspot Minimum, *Space Sci. Rev.*, **93**, 411-472, 2000.

Fludra, A., G. Del Zanna, and B. J. I. Bromage, EUV Observations above Polar Coronal Holes, *Space Sci. Rev.*, **87**, 185-188, 1999.

Geiss, J., G. Gloeckler, R. von Steiger, H. Balsiger, L. A. Fisk, et al., The Southern High-Speed Stream: Results from the SWICS Instrument on Ulysses, *Science*, **268**, 1033-1036, 1995.

Giordano, S., E. Antonucci, G. Noci, M. Romoli, and J. L. Kohl, Identification of the Coronal Sources of the Fast Solar Wind, *Astrophys. J.*, **531**, L79-L82, 2000.

Hassler, D. M., I. E. Dammasch, P. Lemaire, P. Brekke, W. Curdt, et al., Solar Wind Outflow and the Chromospheric Magnetic Network, *Science*, **283**, 810-813, 1999.

Insley, J. E., V. Moore, and R. A. Harrison, First Observations of Coronal Hole Structure and Evolution Using SOHO-CDS, *Solar Phys.*, **175**, 437-456, 1997.

Kohl, J. L., G. Noci, E. Antonucci, G. Tondello, M. C. E. Huber, et al., First Results from the SOHO Ultraviolet Coronagraph Spectrometer, *Solar Phys.*, **175**, 613-644, 1997.

Kohl, J. L., S. Fineschi, R. Esser, A. Ciaravella, S. R. Cranmer, et al., UVCS/SOHO Observations of Spectral Line Profiles in Polar Coronal Holes, *Space Sci. Rev.*, **87**, 233-236, 1999a.

Kohl, J. L., R. Esser, S. R. Cranmer, S. Fineschi, L. D. Gardner, et al., EUV Spectral Line Profiles in Polar Coronal Holes from 1.3 to 3.0 $R_\odot$, *Astrophys. J.*, **510**, L59-L62, 1999b.

Krieger, A. S., A. F. Timothy, and E. C. Roelof, A Coronal Hole and its Identification as the Source of a High Velocity Solar Wind Stream, *Solar Phys.*, **29**, 505-525, 1973.

Lemaire, P., K. Wilhelm, W. Curdt, U. Schühle, E. Marsch, et al., First Results of the SUMER Telescope and Spectrometer on SOHO, II. Imagery and Data Management, *Solar Phys.*, **170**, 105-122, 1997.

Lemaire, P., K. Bocchialini, V. Aletti, D. Hassler, and K. Wilhelm, Search for Signatures of a Coronal Hole in Transition Region Lines Near Disk Center, *Space Sci. Rev.*, **87**, 249-252, 1999.

Stucki, K., S. K. Solanki, I. Rüedi, J. O. Stenflo, A. Brkovic, et al., Coronal Holes Versus Normal Quiet Sun Observed with SUMER, *Astrophys. Space Sci.*, **264**, 53-61, 1999.

Wilhelm, K., The Darkest Regions of Solar Polar Coronal Holes Observed by SUMER on SOHO, *Astrophys. Space Sci.*, **264**, 43-52, 1999.

Wilhelm, K., W. Curdt, E. Marsch, U. Schühle, P. Lemaire, et al., SUMER – Solar Ultraviolet Measurements of Emitted Radiation, *Solar Phys.*, **162**, 189-231, 1995.

Wilhelm, K., P. Lemaire, W. Curdt, U. Schühle, E. Marsch, et al., First Results of the SUMER Telescope and Spectrometer on SOHO, I. Spectra and Spectroradiometry, *Solar Phys.*, **170**, 75-104, 1997.

Wilhelm, K., E. Marsch, B. N. Dwivedi, D. M. Hassler, P. Lemaire, et al., The Solar Corona Above Polar Coronal Holes as Seen by SUMER on SOHO, *Astrophys. J.*, **500**, 1023-1038, 1998.

Wilhelm, K., I. E. Dammasch, E. Marsch, and D. M. Hassler, On the Source Regions of the Fast Solar Wind in Polar Coronal Holes, *Astron. Astrophys.*, **353**, 749-756, 2000.

Woch, J., W. I. Axford, U. Mall, B. Wilken, S. Livi, et al., SWICS/Ulysses Observations: The Three-Dimensional Structure of the Heliosphere in the Declining/Minimum Phase of the Solar Cycle, *Geophys. Res. Lett.*, **24**, 2885-2888, 1997.